Experimental Study of the Infrared Characteristic of a Small Turbojet Engine

Bonchan Gu*, Seung Wook Baek**, Hyunwook Jegal***, Seongman Choi****, and Won Cheol Kim*****

*Korea Advanced Institute of Science and Technology

291 Daehak-ro, Yuseong-gu, Daejeon, 3414, Republic of Korea

**Korea Advanced Institute of Science and Technology

291 Daehak-ro, Yuseong-gu, Daejeon, 3414, Republic of Korea

***Korea Advanced Institute of Science and Technology

291 Daehak-ro, Yuseong-gu, Daejeon, 3414, Republic of Korea

****Chonbuk National University

567 Baekje-daero, Deokjin-Gu, Jeonju-si, Jeollabuk-do, 54896, Republic of Korea

*****Agency for Defense Development

Republic of Korea

Abstract

Low observable exhaust nozzles applied to stealth aircrafts suppress infrared (IR) signature compared to a conventional aircraft nozzle. The application of low observable nozzle technology allows further enhancement of aircraft survivability with IR signature suppression by hiding the hot parts of the engine. The present study investigates the characteristic of IR signatures radiated from the exhaust plume of a small turbojet engine. A conventional nozzle and aspect ratio nozzles, which were combined with the small turbojet engine, were designed to compare the IR signatures. The engine operated in the same conditions, and the measurement of IR signature was conducted in the steady state. The kerosene along with the lubricant oil was used as a fuel for the engine. The IR radiation emitted from the small turbojet engine was measured using spectroradiometer in the wide range of 667 cm^{-1} ~ 5000 cm^{-1}. A blackbody was used to calibrate the raw spectrum of the IR signature and thereby comparing with the theoretical values. The experiments revealed that the IR signature characteristics from the exhaust plume of AR nozzles are presented different phenomenon compared with one from the exhaust plume of the circular nozzle. The IR signatures of the AR nozzles were found to be lower than the conventional nozzle, the effects are apparent in the range of 2000 cm^{-1} ~ 2500 cm^{-1}.

1. Introduction

The advantage of the latest fighter aircraft on the battlefield is determined by the level of low observable technology, and it is directly linked to the survivability of the aircraft. Due to the development of increasingly sophisticated and detailed IR detectors, it is a major threat to ensuring the survivability of aircraft from the enemy detection systems. Consequently, reduction of the IR signature from an aircraft is important to enhance the survivability of the aircraft [1]. The sources of IR signatures of an aircraft are surfaces aerodynamically heated, rear fuselage skin heated by engine, exhaust plume, nozzles, engine turbine, and reflection by sunshine and earthshine. The main IR sources are the exhaust plume emission and surface emission of nozzle wall [2]. These signatures are sitting targets for the heat-seeking missiles, so, it is essential to decrease the range of enemy detection by reducing the IR signature emitted from the aircraft.

At present, many experimental studies on the measurement of IR signatures have been conducted to comprehend the IR signature characteristic. S. Cogliandro and P. Castelli [3] investigated the plume IR emission of turboshaft engines in 1-14.5 micron band by using a spectroradiometer with CVF and IR scanners. A. D. Devir et al. [4] studied IR radiation associated with the under expanded exhaust plume by a test-bed facility. These results led to a better understanding of the dominant physical and chemical process governing plume radiation. S. J. P. Retief et al [5] conducted measurements of a micro turbine engine plume in different IR bands within 1 ~ 15 μm. The results presented the usefulness of a cost effective micro turbine engine for concept plume studies related to full scale aircraft plume. The mid-wave IR band is also the most versatile regarding plume observations, although IR emission is detected at

other wavelengths outside this band. In their studies, the measurements were performed to obtain the IR signature of the exhaust plume exited from the nozzle exit in the form of circle called basic nozzle.

As the importance of IR signature reduction has been continuously increased, a number of researches have carried out until recently to suppress the IR emission through changing the shape of the exhaust system. Z. Jingzhou et al. [6] applied IR suppression technologies, which are the lobed mixer ejector and masking box surface and louvers, on helicopter exhaust system. R. Decher [7] numerically analysed the IR emission characteristics for a mixed flow turbofans with aspect ratio nozzles. C. H. An et al. [8] studied the effects of S-shaped nozzle configurations of an unmanned aerial vehicle (UAV) and atmospheric conditions on plume IR signatures. The studies mentioned above were performed by analytic methods, and the experimental study on the shape changes of aircraft nozzles, including the effect of atmospheric absorption, have not been studied yet.

In the present study, the characteristic of IR signatures radiated from the exhaust plume of a small turbojet engine was investigated. Also, a measurement system has been established for recording IR signature emitted from the exhaust plume. The measurement tests were carried out according to the change of aspect ratio (AR) of nozzle exit. A conventional nozzle and AR nozzles, which were combined with the small turbojet engine, were designed to compare the IR signatures. The engine operated in the same conditions, and the measurement of IR signature was conducted in the steady state. The kerosene along with the lubricant oil was used as a fuel for the engine. The IR radiation emitted from the small turbojet engine was measured using spectroradiometer in the wide range of 667 cm^{-1} ~ 5000 cm^{-1}. A blackbody was used to calibrate the raw spectrum of the IR signature and thereby comparing with the theoretical values. The results of IR signatures were analysed in the sub-bands to spectrally observe.

2. Experimental apparatus

2.1 Small turbojet engine

A small turbojet engine under tests is a AMT Netherlands Olympus HP engine. The engine is developed for the propulsion of radio controlled flying airplanes, remote heat and power generators, and auxiliary power units. The cut-out image of Olympus HP engine is shown in figure 1. The engine is composed of a single centrifugal compressor and an axial flow turbine. The combustion chamber is of the annular type, which is fitted with a unique fuel system at low pressure. The engine uses a normal model glow plug for ignition, and it starts using an electric motor installed at the inlet of the engine. The motor is separated from the engine shaft when the exhaust gas temperature (EGT) is over 88 and revolution of the engine exceeds 9 000 RPM. Several types of fuel such as JP-4, kerosene, paraffin, and Jet A-1 can be used. In this research, kerosene used in the military aviation was premixed with 4.5 % Aeroshell 500 turbine oil for lubrication. The fuel is supplied by the fuel pump for ignition at the initial stage, and then by the main fuel pump after engine operation. The fuel supply is controlled by electronic control unit (ECU).
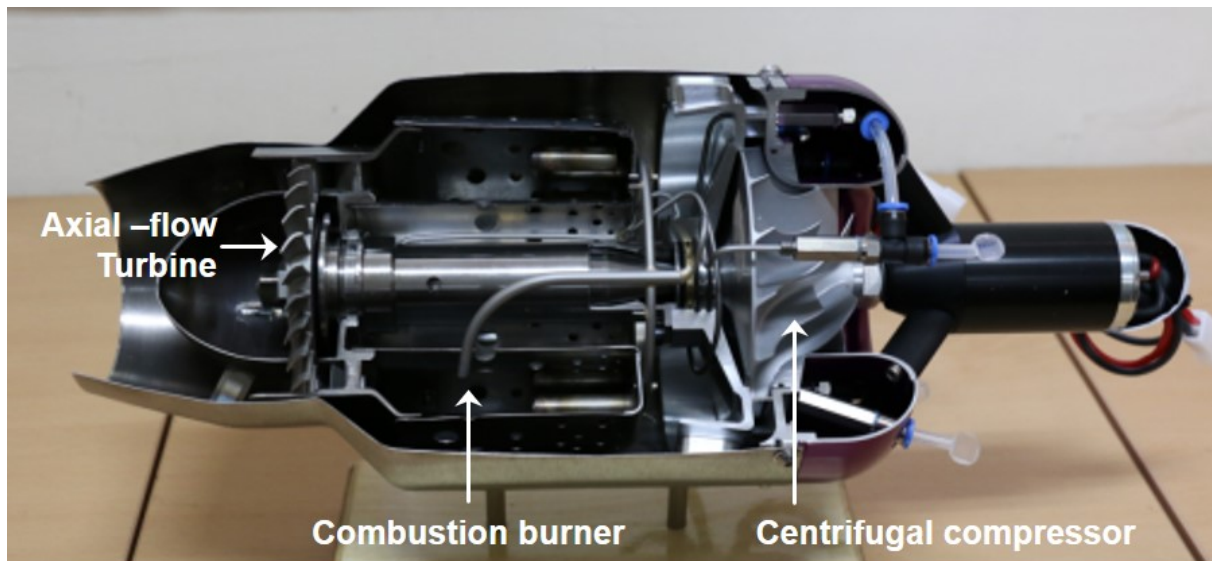
Figure 1: Cut-out of Olympus HP engine

The engine provides a maximum thrust of 230 N at 108 500 RPM. The dimension of the engine is intake diameter of 131 mm and a length of 384 mm. Detailed specifications and performance are presented in the table 1.

Table 1: Specification and performance of the engine

Thrust at maximum RPM, N	230
Thrust at minimum RPM, N	13
Maximum RPM	108 500
Maximum EGT, ℃	750
Mass flow at maximum RPM, g/s	450
Fuel	Kerosene
Pressure ratio at maximum RPM	3.8 : 1

The schematic of the engine test station is illustrated in figure 2. The engine is tightly mounted at a test bed. The sensors used to obtain the data of engine performance were installed in the test bed. The engine operating status is transmitted simultaneously to the engine data terminal and the computer connected to the test bed. The thrust was measured with a load cell, which has an error of 0.06 %. A small turbine flowmeter with a measurement error of 1 % gauged the flow rate of fuel. A RPM sensor located on the impeller blade measured the engine speed. A thermocouple that was a K type (Ni-CR/Ni) was mounted between the turbine and nozzle inlet to get the temperature data of EGT. The temperature was recorded by using a data acquisition product.
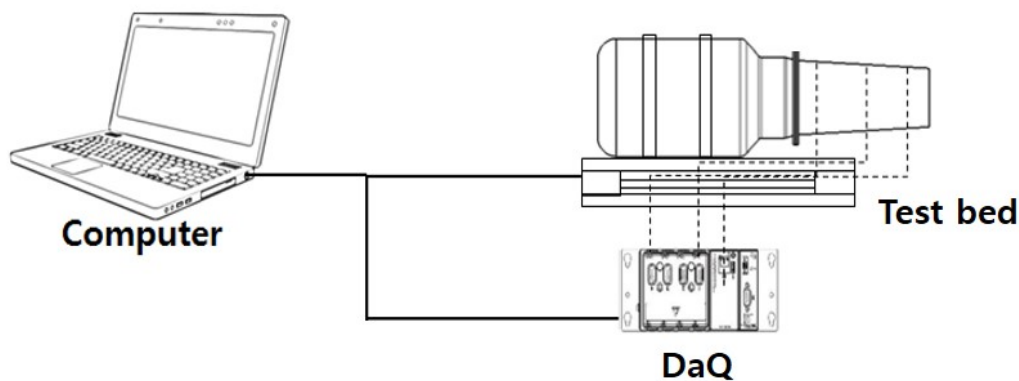
Figure 2: Schematic of engine test station

In order to understand the phenomenon caused by the change of the nozzle exit geometry, the nozzle part of the engine was modified so as to be easily replaceable. Also, to reduce the deformation of the nozzle caused by thermal expansion, the nozzle was designed and manufactured from the same material used for the engine.

2.2 Nozzles

To figure out the influences of nozzle configurations on IR signature from the exhaust plume, two-dimensional shape of nozzle outlet was considered. The dimension of nozzle exit are expressed width and height. The AR of a nozzle exit shape is the ratio of width to height. The aspect ratios of 1, 3, and 5 were considered with a conventional circular exit nozzle. The type of all nozzles were convergent, and the inlet of each nozzle had a circular shape and the same area. In addition, the length of the circular nozzle and AR nozzles are equal to 159. 1 mm. The AR nozzles were designed

in rectangular, but the nozzle outlet of the nozzles had the same area with that of the circular nozzle. Figure 3 shows a circular nozzle and three different AR nozzles.
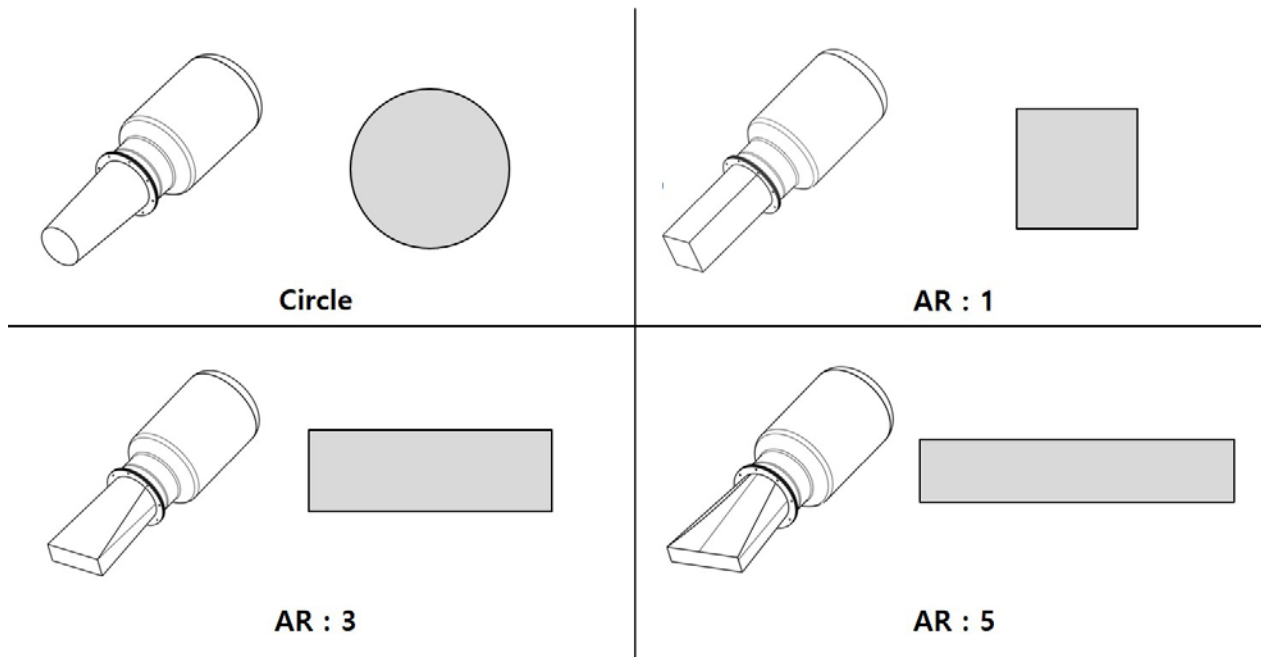
Figure 3: Schematic of a circular nozzle and AR nozzles with nozzle exit shape

Table 2: Dimension of nozzles

Nozzle	Aspect Ratio	Width	Height	Area
		mm	mm	mm^2
Circle	-	Ø 63.2		3137
AR 1	1	56.0	56.0	3136
AR 3	3	97.0	32.3	3133
AR 5	5	125.2	25.0	3130

The dimension, the AR, and the exit area of each nozzle are presented in table 2. The area of each nozzle has constant, whereas the perimeter of nozzle exit were different.

2.3 Radiometric measurements

The IR signatures from the exhaust plume were recorded a spectroradiometer. The instrument is a Fourier Transform IR (FTIR), and collects all wavenumbers in a single sweep of the wishbone composed of a moving mirror and a fixed mirror. After collecting the radiant emission from the targets, the interferogram is digitized. The raw spectrum can be obtained by using the FT function from the interferogram. The spectroradiometer, which is ABB MR170, is shown in figure 4.

Figure 4: Spectroradiometer

The spectroradiometer is made up a telescope, an input collimator, two cooled detectors, and a CCD camera. The instrument is mounted on a tripod, was positioned at a distance of at least 5 m from the centreline axis of the engine considering the safety area and the characteristics of the telescope. The measured signals are transmitted from the electronic module to the laptop through the ethernet cables. The specifications of the spectroradiomter are minutely presented in the table 3.

Table 3: Specifications of spectroradiometer

Spectral range, cm^{-1}	667 ~ 5000
Detectors	InSb & MCT
Spectral resolution, cm^{-1}	2
Input aperture, mm	5.1
Field Of View (FOV), mrad	10.06

The calibration of the raw spectrum of the targets was performed by using a blackbody radiator. The data from the blackbody was measured at the same location and conditions with the targets, and it was used as references. The process of the data reduction called radiometric calibration, determining the spectral radiance at each wavenumber, is expressed by equation 1.

$$R_\eta = M_\eta G_\eta + O_\eta \tag{1}$$

Where η indicates the wavenumber, R_η is the spectral radiance, M_η is the measured radiance, G_η and O_η are the gain and offset, respectively. With this equation it is in position to calculate the instrument response function assuming a linear response that needs a minimum of two blackbody temperatures to solve the calibration equation. After calculating the gain and offset from the blackbody, the measured spectrum of the targets were calibrated by using the above equation.

3. Results

3.1 Engine test

Engine performance tests were performed on the same engine operation conditions for the circular nozzle, AR 1, AR 3, and AR 5 nozzles. The EGT and thrust over the operating time according to the nozzles are shown in figure 5. A large amount of the fuel flowed at the initial stage of the operation caused a sudden EGT rise. After the idling section, the EGT and thrust are constant under the same operating conditions. The EGT and thrust rose due to the combustion of the residual fuel remaining in the engine during the shut down.
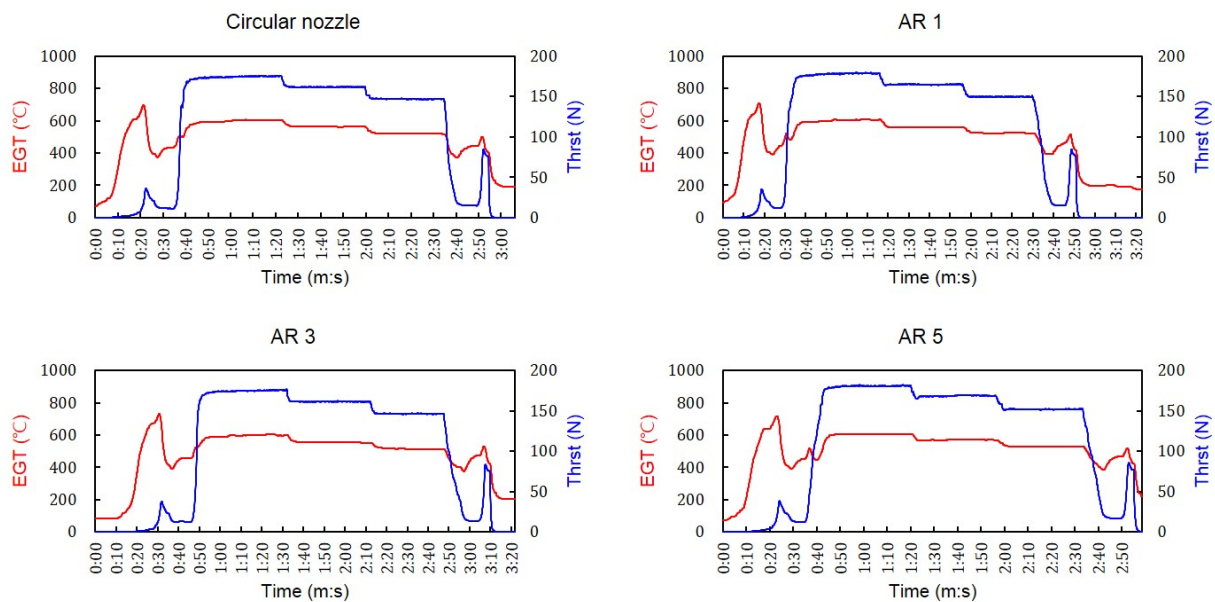
Figure 5: Engine performance according to the nozzles: EGT and thrust

Table 4: Specifications of spectroradiometer

Nozzle	Averaged EGT	Averaged Thrust	Averaged RPM	Averaged Fuel Consumption
	℃	N	%	g/s
Circle	623.30	169.44	97.22	9.14
AR 1	629.71	176.28	96.60	9.12
AR 3	652.26	172.96	96.51	9.03
AR 5	633.07	178.93	96.55	9.25

The measurement of IR signatures were recorded at the first constant steady state. In this section, the averaged results of EGT, thrust, RPM, and fuel consumption for each nozzle are indicated in table 4. The engine performance and operating condition are constant, providing a level of confidence of approximately 96.67 %. Through the tests, it is judged that the influence of the change of nozzles shape on the engine performance was almost insignificant.

3.2 IR signatures

The arrangement of the small turbine engine and the spectroradiometer is shown in figure 6. The target point was 10 cm (D_{exit}) from the nozzle exit on the axis of the engine. The spectroradiometer was positioned at a distance (D) of 5.5 m from the axis of the engine, and the angle was at 90 degrees. The FOV was 10.06 mrad, the diameter (D_{FOV}) of FOV was 53.13 mm, the target area via FOV was 22.2 mm^2, and the solid angle was $7.30 \cdot 10^{-4}$ sr. Air temperature varied from 6.66 ℃ to 8.8 ℃, and air humidity was 55.1 ± 6.2 % at the test location.
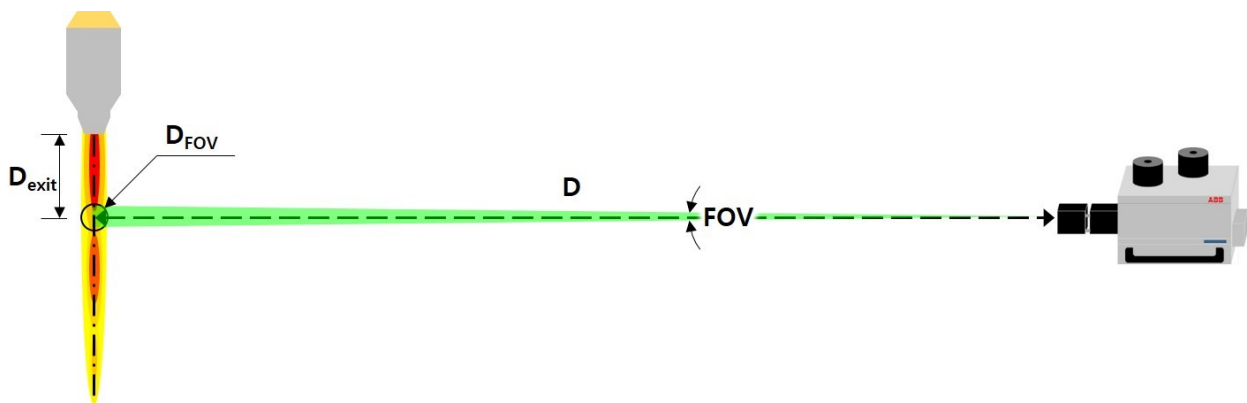
Figure 6: Arrangement of measurement set-up

The strength of the infrared signatures depends on the gas composition and the aspect angle, but is closely related to the temperature of the exhaust plume. Mixing between the hot core part and external air should occur in terms of decrease of temperature. For this reason, the results were analysed how AR influences the IR signatures of exhaust plume in comparison with the circular nozzle. The IR signatures of the exhaust plume of four nozzles, which were measured during engine operation, are presented in figure 7. The spectrum shows the similar signature characteristics regardless of the variation of AR compared with the circular nozzle. In order to figure out the spectral characteristics, the spectral range where the signature was radiated was divided into three bands: 1000 cm^{-1} ~ 2000 cm^{-1} (band 1), 2000 cm^{-1} ~ 2500 cm^{-1} (band 2), and 2500 cm^{-1} ~ 4000 cm^{-1} (band 3). As seen in figure 7, the spectral profile is not affected by the change of nozzles in band 1 and band 3. It can be seen that the spectral radiance decreases at the AR increases at band 2 except for the wavenumber of 2325 cm^{-1} in which carbon dioxide in atmosphere generates the noise. It is implied that the expanded mixing area at high AR causes the reduction of the plume temperature.

Figure 8 illustrate comparison of the spectral radiance considered atmospheric absorption between the nozzles at three bands. In band 2, distinct changes take place in near 2350 cm^{-1}. At this spectral region, the IR signature is strongly absorbed by carbon dioxide irrespective of the nozzles. The spectral region of the radiant emission of the exhaust plume is wider than that of atmospheric absorption, therefore, the red spike at 2290 cm^{-1} and the blue spike at 2390 cm^{-1} are observed. Also, the IR signatures were reduced in proportion to AR because of the plumes were widely distributed like the results in figure 7.

The analysis was quantitatively performed for how much the IR signatures reduced of AR nozzles compared to the circular nozzle. The rate of radiance, is defined as the ratio of the band radiance of all nozzles to the band radiance of circular nozzle, were calculated at the full range and three bands. The results are presented in figure 9. The integrated radiance decreased with increasing AR at the full range, band 1, and band 2. On the other hand, AR 3 and AR 5 of band 3 were increased because the widen plume region heated water vapour in atmosphere. In the band 2, the band radiance was reduced to 27.65 %. Moreover, most of the IR signatures were emitted and the significant changes according to the AR were occurred at the band 2.

Bonchan Gu, Seung Wook Baek, Hyunwook Jegal, Seongman Choi, and Won Cheol Kim
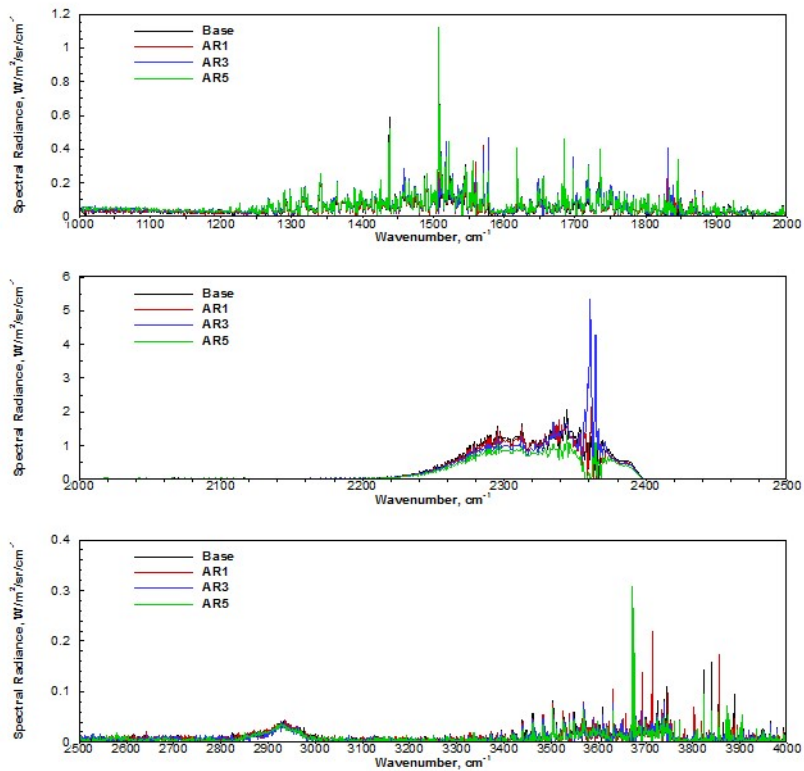
Figure 7: Comparison of the spectral radiance between the nozzles at three bands
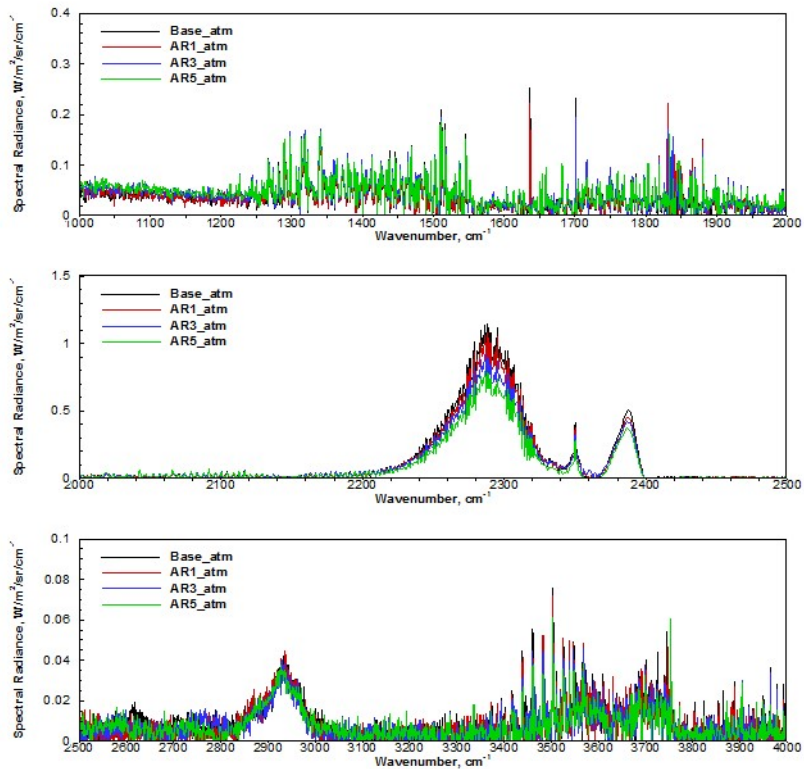
Figure 8: Comparison of the spectral radiance considered atmospheric absorption between the nozzles at three bands
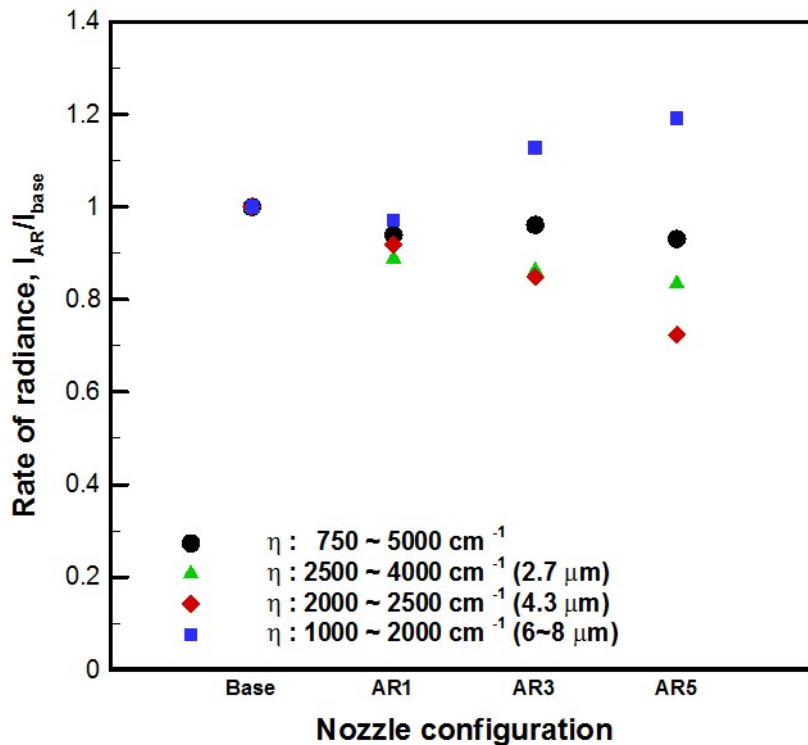
Figure 9: Rate of radiance according to the nozzle configuration

4. Conclusions

The characteristic of IR signatures radiated from the exhaust plume of a small turbojet engine was investigated. The experimental set-up is proper for measurements of IR signature emitted from the exhaust plume. The measurement tests were carried out for a conventional circular nozzle and aspect ratio nozzles, which were combined with the small turbojet engine. The engine operated in the same conditions, and the measurement of IR signature was conducted in the steady state. The radiant emission was measured using spectroradiometer in the wide range of 667 cm^{-1} ~ 5000 cm^{-1}. The results of IR signatures were analysed in the sub-bands to spectrally observe. The spectral radiance decreases at the AR increases at band 2 except for the wavenumber of 2325 cm^{-1}. The IR signature is strongly absorbed by carbon dioxide irrespective of the nozzles at this spectral region. Most of the IR signatures were emitted and the significant changes according to the AR were occurred at the band 2.

Acknowledgements

References

[1] S. P. Mahulikar, H. R. Sonawane, and G. A. Rao. 2007. Infrared signature studies of aerospace vehicles. *Progress in Aerospace Sciences.* 43: 218-245.

[2] S. P. Mahulikar, S. K. Potnuru, and G. A. Rao. 2009. Study of sunshine, skyshine, and earthshine for aircraft infrared detection. *Journal of Optics A: Pure and Applied Optics.*

[3] S. Cogliandro and P. Castelli. 1986. Plume infrared signature measurements and comparison with a theoretical model. *SPIE Vol. 685 Infrared Technology XII.*

[4] A. Devir, A. Lessin, M. Lev, J. Stricker, S. Yaniv, Y. Cohen, Y. Kanelbaum, G. Avital, L. Gamss, J. Macales, B. Trieman, and A. Sternlieb. 2001. Comparison of calculated and measured radiation from a rocket motor plume. *AIAA 2001-0385*.

[5] S. J. P. Retief, M. M. Dreyer, C. Brink. 2014. Infrared recordings for characterizing an aircraft plume. *Proceedings of SPIE – The International Society for Optical Engineering.*

[6] Z. Jingzhou, P. Chengxiong, and S. Yong. 2014. Progress in helicopter infrared signature suppression. *Chinese Journal of Aeronautics.* Vol. 27. No. 2: 189-199.

[7] R. Decher. 1981. Infrared emissions from turbofans with high aspect ratio nozzles. *Journal of aircraft.* Vol. 18. No. 12: 1025-1031.

[8] C. H. An, D. W. Kang, S. T. Baek, R. S. Myong, W. C. Kim, and S. M. Choi. 2016. Analysis of plume infrared signatures of S-shaped nozzle configurations of aerial vehicle. *Journal of Aircraft.* Vol. 53. Issue. 6: 1768-1778.